ARTICLE IN PRESS

Physica B xxx (xxxx) xxx–xxx

Contents lists available at ScienceDirect

Physica B

journal homepage: www.elsevier.com/locate/physb

Magnetization process and low-temperature thermodynamics of a spin-1/2 Heisenberg octahedral chain☆

Jozef Strečka[a,*], Johannes Richter[b], Oleg Derzhko[c,d], Taras Verkholyak[c], Katarína Karľová[a]

[a] Institute of Physics, Faculty of Science, P. J. Šafárik University, Park Angelinum 9, 04001 Košice, Slovakia
[b] Institut für Theoretische Physik, Otto-von-Guericke Universität in Magdeburg, 39016 Magdeburg, Germany
[c] Institute for Condensed Matter Physics, NASU, Svientsitskii Street 1, 79011 L'viv, Ukraine
[d] Department for Theoretical Physics, Ivan Franko National University of L'viv, Drahomanov Street 12, 79005 L'viv, Ukraine

ARTICLE INFO

Keywords:
Heisenberg octahedral chain
Quantum phase transitions
Magnetization plateaus
Thermodynamics

ABSTRACT

Low-temperature magnetization curves and thermodynamics of a spin-1/2 Heisenberg octahedral chain with the intra-plaquette and monomer-plaquette interactions are examined within a two-component lattice-gas model of hard-core monomers, which takes into account all low-lying energy modes in a highly frustrated parameter space involving the monomer-tetramer, localized many-magnon and fully polarized ground states. It is shown that the developed lattice-gas model satisfactorily describes all pronounced features of the low-temperature magnetization process and the magneto-thermodynamics such as abrupt changes of the isothermal magnetization curves, a double-peak structure of the specific heat or a giant magnetocaloric effect.

1. Introduction

One-dimensional quantum Heisenberg spin chains display at low enough temperatures remarkable magnetization curves, which may even basically depend at low magnetic fields on the spin magnitude according to the conjecture made by Haldane [1,2]. Among the most notable features of zero-temperature magnetization curves one could mention fractional magnetization plateaus, quantum spin liquids and macroscopic magnetization jumps, which can be found first of all in frustrated quantum Heisenberg spin models [3,4]. The macroscopic magnetization jumps emergent at a saturation field are closely connected with flat-band physics [5–8] and they can be alternatively viewed as a condensation of localized magnons [3,8–12]. It should be stressed that the localized-magnon picture of the frustrated quantum Heisenberg spin models is of particular importance, because it additionally allows a proper description of low-temperature thermodynamics with the help of simpler classical lattice-gas models projecting out excited states with much higher energy. However, the main drawback of the localized-magnon approach lies in that its validity is usually restricted only to high magnetic fields [3,8–12].

Recently, the localized-magnon approach has been adapted in order to find an exact ground state close to but slightly below saturation field of a spin-$\frac{1}{2}$ Heisenberg octahedral chain, which involves the localized one-magnon state at each elementary square cell (see Fig. 1 for a schematic illustration) [13]. It is worthwhile to remark, moreover, that the spin-$\frac{1}{2}$ Heisenberg octahedral chain exhibits at sufficiently low magnetic fields another exact ground state with the character of the monomer-tetramer phase, which appears due to formation of a singlet state between four spins creating an elementary square plaquette [14]. This singlet-tetramer state can be alternatively considered as the localized two-magnon state, which consequently gives us hope for a proper description of low-temperature thermodynamics of the spin-$\frac{1}{2}$ Heisenberg octahedral chain in a full range of the magnetic fields [13]. In the following, we will develop a novel kind of the localized-magnon approach for the spin-$\frac{1}{2}$ Heisenberg octahedral chain, which indeed provides a consistent description of the low-temperature thermodynamics in a full range of the magnetic fields.

2. Spin-$\frac{1}{2}$ Heisenberg octahedral chain

Let us consider the spin-$\frac{1}{2}$ Heisenberg octahedral chain schematically depicted in Fig. 1(a) and defined through the Hamiltonian

☆ This work was financially supported by the grant of The Ministry of Education, Science, Research and Sport of the Slovak Republic under the contracts Nos. APVV-0097-12 and APVV-14-0076 by the grant of the Slovak Research and Development Agency under the contract No. APVV-14-0073. O.D. and J.R. acknowledge the support by the Deutsche Forschungsgemeinschaft (project RI615/21-2). O.D. was partially supported by Project FF-30F (No. 0116U001539) from the Ministry of Education and Science of Ukraine.

* Corresponding author.
E-mail address: jozef.strecka@upjs.sk (J. Strečka).

http://dx.doi.org/10.1016/j.physb.2017.09.118
Received 19 June 2017; Received in revised form 21 September 2017; Accepted 27 September 2017
0921-4526/

Please cite this article as: Strecka, J., Physica B (2017), http://dx.doi.org/10.1016/j.physb.2017.09.118

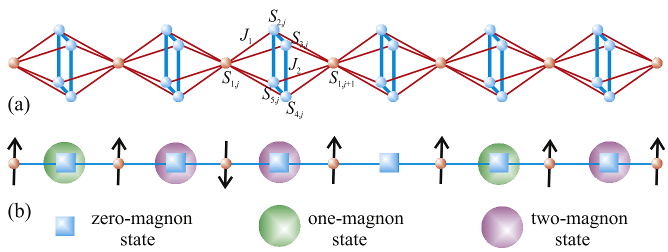

Fig. 1. (a) A schematic representation of the spin-$\frac{1}{2}$ Heisenberg octahedral chain. Thick (blue) lines represent the Heisenberg intra-plaquette coupling J_2, while thin (red) lines correspond to the monomer-plaquette coupling J_1; (b) an equivalent two-component lattice-gas model of hard-core monomers valid in a highly frustrated region $J_2 \geq 2J_1$. Green and violet balls denote hard-core monomers, which represent one-magnon and two-magnon states of square plaquettes given by Eqs. (5) and (6). Unoccupied blue squares denote fully polarized (zero-magnon) state of square plaquettes.

$$\begin{aligned}\hat{\mathcal{H}} = \sum_{j=1}^{N} \Bigg[& J_1(\hat{\boldsymbol{S}}_{1,j} + \hat{\boldsymbol{S}}_{1,j+1})\cdot(\hat{\boldsymbol{S}}_{2,j} + \hat{\boldsymbol{S}}_{3,j} + \hat{\boldsymbol{S}}_{4,j} + \hat{\boldsymbol{S}}_{5,j}) \\ & + J_2(\hat{\boldsymbol{S}}_{2,j}\cdot\hat{\boldsymbol{S}}_{3,j} + \hat{\boldsymbol{S}}_{3,j}\cdot\hat{\boldsymbol{S}}_{4,j} + \hat{\boldsymbol{S}}_{4,j}\cdot\hat{\boldsymbol{S}}_{5,j} + \hat{\boldsymbol{S}}_{5,j}\cdot\hat{\boldsymbol{S}}_{2,j}) \\ & - h\sum_{i=1}^{5} \hat{S}_{i,j}^{z} \Bigg], \end{aligned} \tag{1}$$

where $\hat{\boldsymbol{S}}_{i,j} \equiv (\hat{S}_{i,j}^x, \hat{S}_{i,j}^y, \hat{S}_{i,j}^z)$ stands for a spin-$\frac{1}{2}$ operator at a lattice site given by two subscripts, the former subscript determines a position within the unit cell and the latter subscript the unit cell itself. The parameter J_1 denotes the Heisenberg coupling between nearest-neighbour spins from the monomeric and square-plaquette sites, the parameter J_2 labels the Heisenberg coupling between nearest-neighbour spins from the same square plaquette and the Zeeman term $h \geq 0$ refers to a magnetostatic energy of relevant magnetic moments in a magnetic field. The translational invariance is achieved by the choice of a periodic boundary condition $\boldsymbol{S}_{1,N+1} \equiv \boldsymbol{S}_{1,1}$.

It has been shown in our preceding work that the spin-$\frac{1}{2}$ Heisenberg octahedral chain given by the Hamiltonian (1) can be solved by several complementary analytical and numerical approaches [13], whereas a few unconventional quantum ground states can be corroborated even by exact means. In a low-field part $h \leq J_1 + J_2$ of the highly frustrated parameter space $J_2 \geq 2J_1$ one may for instance employ the variational approach in order to find an exact monomer-tetramer ground state

$$|\mathrm{MT}\rangle = \prod_{j=1}^{N} |\uparrow_{1,j}\rangle \otimes \left[\frac{1}{\sqrt{3}}(|\uparrow_{2,j}\downarrow_{3,j}\uparrow_{4,j}\downarrow_{5,j}\rangle + |\downarrow_{2,j}\uparrow_{3,j}\downarrow_{4,j}\uparrow_{5,j}\rangle) - \frac{1}{\sqrt{12}}(|\uparrow_{2,j}\uparrow_{3,j}\downarrow_{4,j}\downarrow_{5,j}\rangle + |\uparrow_{2,j}\downarrow_{3,j}\downarrow_{4,j}\uparrow_{5,j}\rangle + |\downarrow_{2,j}\uparrow_{3,j}\uparrow_{4,j}\downarrow_{5,j}\rangle + |\downarrow_{2,j}\downarrow_{3,j}\uparrow_{4,j}\uparrow_{5,j}\rangle)\right]. \tag{2}$$

On the other hand, the localized-magnon approach [8–12] can be adapted in order to afford an exact evidence of the localized many-magnon ground state

$$|\mathrm{LM}\rangle = \prod_{j=1}^{N} |\uparrow_{1,j}\rangle \otimes \frac{1}{2}(|\downarrow_{2,j}\uparrow_{3,j}\uparrow_{4,j}\uparrow_{5,j}\rangle - |\uparrow_{2,j}\downarrow_{3,j}\uparrow_{4,j}\uparrow_{5,j}\rangle + |\uparrow_{2,j}\uparrow_{3,j}\downarrow_{4,j}\uparrow_{5,j}\rangle - |\uparrow_{2,j}\uparrow_{3,j}\uparrow_{4,j}\downarrow_{5,j}\rangle), \tag{3}$$

which appears in the highly frustrated region $J_2 \geq 2J_1$ at moderate values of the magnetic field $J_1 + J_2 \leq h \leq J_1 + 2J_2$. Of course, the classical ferromagnetic state

$$|\mathrm{FM}\rangle = \prod_{j=1}^{N} |\uparrow_{1,j}\uparrow_{2,j}\uparrow_{3,j}\uparrow_{4,j}\uparrow_{5,j}\rangle \tag{4}$$

becomes an exact ground state for the magnetic fields higher than the saturation value $h_s = J_1 + 2J_2$. The primary goal of the present work is to develop in the highly-frustrated region $J_2 \geq 2J_1$ an effective lattice-gas model, which will comprehensively describe the low-temperature magnetization process and thermodynamics.

3. Lattice-gas model of hard-core monomers

The many-magnon ground state (3) emergent below the saturation field involves except fully polarized monomeric spins a single localized magnon trapped at each elementary square plaquette as given by the eigenvector

$$|1\rangle_j = \frac{1}{2}(|\downarrow_{2,j}\uparrow_{3,j}\uparrow_{4,j}\uparrow_{5,j}\rangle - |\uparrow_{2,j}\downarrow_{3,j}\uparrow_{4,j}\uparrow_{5,j}\rangle + |\uparrow_{2,j}\uparrow_{3,j}\downarrow_{4,j}\uparrow_{5,j}\rangle - |\uparrow_{2,j}\uparrow_{3,j}\uparrow_{4,j}\downarrow_{5,j}\rangle). \tag{5}$$

Contrary to this, the monomer-tetramer ground state (2) is constituted by a singlet-tetramer state of the four spins forming an elementary square plaquette, which can be alternatively viewed as the localized two-magnon state given by the eigenvector

$$\begin{aligned}|2\rangle_j = & \frac{1}{\sqrt{3}}(|\uparrow_{2,j}\downarrow_{3,j}\uparrow_{4,j}\downarrow_{5,j}\rangle + |\downarrow_{2,j}\uparrow_{3,j}\downarrow_{4,j}\uparrow_{5,j}\rangle) \\ & - \frac{1}{\sqrt{12}}(|\uparrow_{2,j}\uparrow_{3,j}\downarrow_{4,j}\downarrow_{5,j}\rangle + |\uparrow_{2,j}\downarrow_{3,j}\downarrow_{4,j}\uparrow_{5,j}\rangle + |\downarrow_{2,j}\uparrow_{3,j}\uparrow_{4,j}\downarrow_{5,j}\rangle \\ & + |\downarrow_{2,j}\downarrow_{3,j}\uparrow_{4,j}\uparrow_{5,j}\rangle). \end{aligned} \tag{6}$$

It is noteworthy that the monomeric spins $S_{1,j}$ are effectively decoupled from the four spins forming the singlet-tetramer state (6). To summarize, the four spins forming a square plaquette display in the highly frustrated region $J_2 \geq 2J_1$ either the localized one-magnon state (5) or the localized two-magnon state (6) or are fully polarized within all available lowest-energy eigenstates of the spin-$\frac{1}{2}$ Heisenberg octahedral chain, while the monomeric spins are always fully polarized except that they are surrounded by two square plaquettes in the singlet-tetramer state (6) due to the effective decoupling of the monomer-plaquette interaction J_1.

Bearing this in mind, the low-temperature magnetization process and thermodynamics of the spin-$\frac{1}{2}$ Heisenberg octahedral chain can be reformulated as a two-component lattice-gas model of hard-core monomers (see Fig. 1(b) for a schematic illustration), since each square plaquette can host either one localized one-magnon state (5) represented by the first kind of hard-core monomers with the chemical potential $\mu_1 = J_1 + 2J_2 - h$ or one localized two-magnon state (6) represented by the second kind of hard-core monomers with the